PHYSICAL REVIEW D **82,** 073015 (2010)

Parallel hybrid textures of lepton mass matrices

S. Dev,* Shivani Gupta,† and Radha Raman Gautam‡

Department of Physics, Himachal Pradesh University, Shimla 171005, India

(Received 8 June 2010; published 29 October 2010)

We analyze the parallel hybrid texture structures in the charged lepton and the neutrino sector. These parallel hybrid texture structures have physical implications as they cannot be obtained from arbitrary lepton mass matrices through weak basis transformations. The total 60 parallel hybrid texture structures can be grouped into 12 classes, and all the hybrid textures in the same class have identical physical implications. We examine all 12 classes under the assumption of nonfactorizable phases in the neutrino mass matrix. Five out of the total 12 classes are found to be phenomenologically disallowed. We study the phenomenological implications of the allowed classes for 1–3 mixing angle, Majorana and Dirac-type *CP* violating phases. Interesting constraints on effective Majorana mass are obtained for all the allowed classes.

DOI: 10.1103/PhysRevD.82.073015 PACS numbers: 14.60.Pq

I. INTRODUCTION

The origin of fermion masses and mixing apart from *CP* violation remains one of the least understood aspects of the standard model (SM) of fundamental particle interactions. In the SM, fermion masses and mixing angles are free parameters and span a wide range of values and, to accommodate such a diverse mass spectrum, the Yukawa couplings must span over 5 orders of magnitude. In the SM, neutrinos are massless but experiments performed during the last two decades have established that neutrinos have small but nonvanishing masses which leads to a further increase in the number of free parameters. Thus, the main theoretical challenges are to reduce the number of free parameters in the Yukawa sector and to obtain tiny neutrino masses but large mixing angles. The proposals aimed at reducing the number of free parameters and, thereby, restricting the form of the mass matrices include the presence of texture zeros [1–6], requirement of zero determinant [7], and the zero trace condition [8]. In addition, the presence of vanishing minors [9] and the simultaneous existence of a texture zero and a vanishing minor have recently [10] been investigated. Attempts have been made to understand the observed pattern of quark/lepton masses and mixings by introducing flavor symmetries (Abelian as well as non-Abelian) which naturally leads to such texture structures. To be more specific, texture zeros and flavor symmetries have yielded quantitative relationships between fermion mass ratios and flavor mixing angles. A unified description of flavor physics and *CP* violation in the quark/lepton sectors can be achieved by constructing a low-energy effective theory with the SM gauge symmetry and some discrete non-Abelian family symmetry and, subsequently, embedding this theory into grand unified theory (GUT) models like SO(10) [11]. The search for an adequate discrete symmetry has mainly focused on the minimal subgroups of SO(3) or SU(3) with at least one singlet and one doublet irreducible representation to accommodate the fermions belonging to each generation. One such subgroup, for example, is the quaternion group Q_8 [12] which not only accommodates the three generations of fermions but also explains the rather large difference between the values of the 2–3 mixing in the quark and lepton sectors. Quaternion symmetry like some other discrete symmetries leads to nontrivial relationships among the nonvanishing elements of the mass matrix. Such textures with equalities between different elements along with some vanishing elements have been referred to as hybrid textures. Detailed phenomenological analyses of hybrid textures with one texture zero and an equality in the neutrino mass matrix in the flavor basis have been reported [13] earlier. However, the investigation of the neutrino mass matrix in the diagonal charged lepton basis can only be regarded as a precursor of a more general study where both the charged lepton and the neutrino mass matrices are nondiagonal.

In the present work, we examine the implications of parallel hybrid texture structures of both the charged lepton and the neutrino mass matrices in a nondiagonal basis assuming the charged lepton mass matrices to be Hermitian. However, it is pertinent to emphasize here that Hermitian charged lepton mass matrices cannot be obtained within the framework of the standard electroweak gauge group. Furthermore, parallel hybrid texture structures for lepton mass matrices can only be ensured by imposing discrete non-Abelian lepton flavor symmetries. There exist a rather large (sixty to be precise [Table I]) number of possible hybrid textures with one texture zero and one equality between mass matrix elements. However, we find that these 60 hybrid texture structures can be grouped into 12 classes such that all the hybrid textures

*dev5703@yahoo.com
†shiroberts_1980@yahoo.co.in
‡gautamrrg@gmail.com

TABLE I. All possible parallel hybrid texture structures. The hybrid textures in a class have the same physical implications.

Class	A	B	C	D	E	F
I	$\begin{pmatrix} a & b & 0 \\ & a & e \\ & & f \end{pmatrix}$	$\begin{pmatrix} a & b & c \\ & a & 0 \\ & & f \end{pmatrix}$	$\begin{pmatrix} a & 0 & c \\ & d & e \\ & & a \end{pmatrix}$	$\begin{pmatrix} a & b & c \\ & d & 0 \\ & & a \end{pmatrix}$	$\begin{pmatrix} a & 0 & c \\ & d & e \\ & & d \end{pmatrix}$	$\begin{pmatrix} a & b & 0 \\ & d & e \\ & & d \end{pmatrix}$
II	$\begin{pmatrix} 0 & b & c \\ & d & e \\ & & d \end{pmatrix}$	$\begin{pmatrix} a & b & c \\ & 0 & e \\ & & a \end{pmatrix}$	$\begin{pmatrix} a & b & c \\ & a & e \\ & & 0 \end{pmatrix}$			
III	$\begin{pmatrix} 0 & b & b \\ & d & e \\ & & f \end{pmatrix}$	$\begin{pmatrix} a & b & c \\ & 0 & c \\ & & f \end{pmatrix}$	$\begin{pmatrix} a & b & c \\ & d & c \\ & & 0 \end{pmatrix}$			
IV	$\begin{pmatrix} a & a & c \\ & 0 & e \\ & & f \end{pmatrix}$	$\begin{pmatrix} a & b & a \\ & d & e \\ & & 0 \end{pmatrix}$	$\begin{pmatrix} 0 & b & c \\ & b & e \\ & & f \end{pmatrix}$	$\begin{pmatrix} a & b & c \\ & d & d \\ & & 0 \end{pmatrix}$	$\begin{pmatrix} 0 & b & c \\ & d & e \\ & & c \end{pmatrix}$	$\begin{pmatrix} a & b & c \\ & 0 & e \\ & & e \end{pmatrix}$
V	$\begin{pmatrix} a & a & c \\ & d & e \\ & & 0 \end{pmatrix}$	$\begin{pmatrix} a & b & a \\ & 0 & e \\ & & f \end{pmatrix}$	$\begin{pmatrix} a & b & c \\ & b & e \\ & & 0 \end{pmatrix}$	$\begin{pmatrix} 0 & b & c \\ & d & d \\ & & f \end{pmatrix}$	$\begin{pmatrix} a & b & c \\ & 0 & e \\ & & f \end{pmatrix}$	$\begin{pmatrix} 0 & b & c \\ & d & e \\ & & e \end{pmatrix}$
VI	$\begin{pmatrix} a & b & c \\ & 0 & a \\ & & c \end{pmatrix}$	$\begin{pmatrix} a & b & c \\ & d & a \\ & & 0 \end{pmatrix}$	$\begin{pmatrix} 0 & b & c \\ & c & e \\ & & f \end{pmatrix}$	$\begin{pmatrix} a & b & c \\ & c & e \\ & & 0 \end{pmatrix}$	$\begin{pmatrix} 0 & b & c \\ & d & e \\ & & b \end{pmatrix}$	$\begin{pmatrix} a & b & c \\ & c & e \\ & & 0 \end{pmatrix}$
VII	$\begin{pmatrix} a & a & 0 \\ & d & e \\ & & f \end{pmatrix}$	$\begin{pmatrix} a & 0 & a \\ & d & e \\ & & f \end{pmatrix}$	$\begin{pmatrix} a & b & c \\ & b & 0 \\ & & f \end{pmatrix}$	$\begin{pmatrix} a & 0 & c \\ & d & d \\ & & f \end{pmatrix}$	$\begin{pmatrix} a & b & c \\ & d & 0 \\ & & c \end{pmatrix}$	$\begin{pmatrix} a & b & 0 \\ & d & e \\ & & e \end{pmatrix}$
VIII	$\begin{pmatrix} a & b & c \\ & d & 0 \\ & & d \end{pmatrix}$	$\begin{pmatrix} a & b & 0 \\ & d & e \\ & & a \end{pmatrix}$	$\begin{pmatrix} a & 0 & c \\ & a & e \\ & & f \end{pmatrix}$			
IX	$\begin{pmatrix} a & b & b \\ & d & 0 \\ & & f \end{pmatrix}$	$\begin{pmatrix} a & b & 0 \\ & d & b \\ & & f \end{pmatrix}$	$\begin{pmatrix} a & 0 & c \\ & d & c \\ & & f \end{pmatrix}$			
X	$\begin{pmatrix} a & b & b \\ & 0 & e \\ & & f \end{pmatrix}$	$\begin{pmatrix} a & b & b \\ & d & e \\ & & 0 \end{pmatrix}$	$\begin{pmatrix} 0 & b & c \\ & d & b \\ & & f \end{pmatrix}$	$\begin{pmatrix} a & b & c \\ & d & b \\ & & f \end{pmatrix}$	$\begin{pmatrix} 0 & b & c \\ & d & c \\ & & f \end{pmatrix}$	$\begin{pmatrix} a & b & c \\ & 0 & c \\ & & f \end{pmatrix}$
XI	$\begin{pmatrix} a & a & c \\ & d & 0 \\ & & f \end{pmatrix}$	$\begin{pmatrix} a & b & a \\ & d & 0 \\ & & f \end{pmatrix}$	$\begin{pmatrix} a & b & 0 \\ & b & e \\ & & f \end{pmatrix}$	$\begin{pmatrix} a & b & 0 \\ & d & d \\ & & f \end{pmatrix}$	$\begin{pmatrix} a & 0 & c \\ & d & e \\ & & c \end{pmatrix}$	$\begin{pmatrix} a & 0 & c \\ & d & e \\ & & e \end{pmatrix}$
XII	$\begin{pmatrix} a & 0 & c \\ & d & a \\ & & f \end{pmatrix}$	$\begin{pmatrix} a & b & 0 \\ & d & a \\ & & f \end{pmatrix}$	$\begin{pmatrix} a & 0 & c \\ & c & e \\ & & f \end{pmatrix}$	$\begin{pmatrix} a & b & c \\ & c & 0 \\ & & f \end{pmatrix}$	$\begin{pmatrix} a & b & 0 \\ & d & e \\ & & b \end{pmatrix}$	$\begin{pmatrix} a & b & c \\ & d & 0 \\ & & b \end{pmatrix}$

belonging to a particular class have the same physical implications. We examine the phenomenological implications of all 12 classes of neutrino mass matrices with hybrid texture structure under the assumption of nonfactorizable phases in the neutrino mass matrix.

The CP violation in neutrino oscillation experiments can be described through a rephasing invariant quantity J_{CP} [14] with $J_{CP} = \mathrm{Im}(U_{e1}U_{\mu 2}U^*_{e2}U^*_{\mu 1})$. In the parametrization adopted here, J_{CP} is given by

$$J_{CP} = s_{12}s_{23}s_{13}c_{12}c_{23}c^2_{13}\sin\delta. \qquad (1)$$

The effective Majorana mass of the electron neutrino M_{ee} which determines the rate of neutrinoless double beta decay is given by

$$M_{ee} = |m_1c^2_{12}c^2_{13} + m_2s^2_{12}c^2_{13}e^{2i\alpha} + m_3s^2_{13}e^{2i\beta}|. \qquad (2)$$

This important parameter will help decide the nature of neutrinos. The analysis of M_{ee} will be significant as many neutrinoless double beta decay experiments will constrain this parameter. A stringent constraint $|M_{ee}| <$ 0.35 eV was obtained by the ^{76}Ge Heidelberg-Moscow experiment [15]. There is a large number of projects such as SuperNEMO [16], CUORE [17], CUORICINO [17], and GERDA [18] which aim to achieve a sensitivity below 0.01 eV to M_{ee}. Forthcoming experiment SuperNEMO, in particular, will explore $M_{ee} < 0.05$ eV [19]. The experimental constraints on the neutrino parameters at 1, 2 and 3σ [20] are given below:

$$\Delta m_{12}^2 = 7.67^{(+0.16,+0.34,+0.52)}_{(-0.19,-0.36,-0.53)} \times 10^{-5}\ \text{eV}^2,$$
$$\Delta m_{23}^2 = \pm 2.39^{(+0.11,+0.27,+0.47)}_{(-0.8,-0.20,-0.33)} \times 10^{-3}\ \text{eV}^2,$$
$$\theta_{12} = 33.96^{\circ(+1.16,+2.43,+3.80)}_{(-1.12,-2.13,-3.10)}, \tag{3}$$
$$\theta_{23} = 43.05^{\circ(+4.18,+7.83,+10.32)}_{(-3.35,-5.82,-7.93)},$$
$$\theta_{13} < 12.38^\circ (3\sigma).$$

The upper bound on θ_{13} is given by the CHOOZ experiment.

II. WEAK BASIS TRANSFORMATIONS

Assuming neutrinos to be of Majorana nature, the most general weak basis transformation (under which lepton mass matrices change but which leaves the gauge currents invariant) is

$$M_l \to M_l' = W^\dagger M_l W', \qquad M_\nu \to M_\nu' = W^T M_\nu W, \tag{4}$$

where W and W' are 3×3 unitary matrices and M_l, M_ν are the charged lepton and the neutrino mass matrices, respectively.

A. Parallel hybrid texture structures

In this section we investigate the possibility of obtaining parallel hybrid texture structures starting from an arbitrary Hermitian charged lepton and complex symmetric neutrino mass matrix. We follow the line of argument advanced by Branco *et al.* [21] for parallel four texture zero Ansätze. For illustration we choose a specific hybrid texture structure (IA) (Table I) with a zero at the (1, 3) position and equality of (1, 1) and (2, 2) elements:

$$M_l = \begin{pmatrix} a_l & b_l & 0 \\ b_l^* & a_l & e_l \\ 0 & e_l^* & f_l \end{pmatrix}, \qquad M_\nu = \begin{pmatrix} a_\nu & b_\nu & 0 \\ b_\nu & a_\nu & e_\nu \\ 0 & e_\nu & f_\nu \end{pmatrix}, \tag{5}$$

where M_l is Hermitian and M_ν is complex symmetric. We can rephase M_l and M_ν such that

$$M_l \to X^\dagger M_l X, \qquad M_\nu \to X^T M_\nu X, \tag{6}$$

where $X \equiv \text{diag}(e^{i\phi_1}, e^{i\phi_2}, e^{i\phi_3})$ and we can choose ϕ_i such that M_l becomes real. We can use the remaining freedom to remove one phase from M_ν. It is instructive to enumerate the number of free parameters in the above two parallel hybrid texture structures. The charged lepton mass matrix after rephasing is left with four real parameters. There are seven free parameters in the neutrino mass matrix (four real parameters and three phases). In total, we have 11 free parameters in M_l and M_ν whereas in the leptonic sector considering neutrinos to be Majorana particles there are 12 physical parameters (six lepton masses, three mixing angles, and three phases) for three generations of neutrinos. Thus, starting from an arbitrary Hermitian M_l and complex symmetric M_ν, we cannot obtain parallel hybrid texture structures through weak basis transformations as the number of free parameters for such texture structures is less than 12. This implies that these parallel texture structures have physical implications. However, if the condition of Hermiticity in M_l is removed then these parallel texture structures can be obtained through weak basis transformations and will, thus, have no physical implications as the total number of free parameters now in M_l and M_ν is greater than 12. In our analysis, we consider M_l to be Hermitian.

B. Weak basis equivalent classes of hybrid textures

Different parallel hybrid texture structures of the charged lepton and neutrino mass matrices can be related by a weak basis transformation. The implications of these hybrid textures which are related by such a transformation are exactly the same. This weak basis transformation can be performed by a permutation matrix P as

$$M_l' = P^T M_l P, \qquad M_\nu' = P^T M_\nu P, \tag{7}$$

which changes the position of the texture zero and an equality but preserves the parallel structure of charged lepton and neutrino mass matrices. The permutation matrix P belongs to the group of six permutation matrices. We find that all 60 hybrid textures (Table I) fall into 12 distinct classes when operated by these permutation matrices. The different classes are shown in Table I. However, this type of classification is not possible in the flavor basis [13] because such a weak basis transformation will render M_l nondiagonal.

III. COMPREHENSIVE ANALYSIS OF DIFFERENT CLASSES OF HYBRID TEXTURES

A. Class I

All the information regarding lepton masses and mixings is encoded in the Hermitian charged lepton mass matrix M_l and the complex symmetric neutrino mass matrix M_ν. First, we analyze the hybrid texture structure in which M_l and M_ν have the parallel structure with equal (1, 1) and (2, 2) elements and a texture zero at the (1, 3) position (case IA). We study this hybrid texture under the assumption of nonfactorizable phases in the neutrino mass matrix M_ν, as it is not always possible to factorize all the phases present in a general complex symmetric mass matrix without unnatural fine-tuning of phases [22]. Therefore, M_l and M_ν are given by

$$M_l = \begin{pmatrix} a_l & b_l & 0 \\ b_l^* & a_l & e_l \\ 0 & e_l^* & f_l \end{pmatrix}, \qquad M_\nu = \begin{pmatrix} a_\nu & b_\nu & 0 \\ b_\nu & a_\nu & e_\nu \\ 0 & e_\nu & f_\nu \end{pmatrix}, \tag{8}$$

respectively. The Hermiticity of M_l requires its diagonal elements a_l and f_l to be real whereas the nondiagonal elements b_l and e_l are in general complex, i.e., $b_l = |b_l|e^{i\phi_1}$, $e_l = |e_l|e^{i\phi_2}$. All the nonvanishing elements of M_ν are, in general, complex. The charged lepton mass matrix M_l can be diagonalized by the unitary transformation

$$M_l = V_l M_l^d V_l^\dagger, \tag{9}$$

where $V_l^\dagger = V_l^{-1}$. The Hermitian matrix M_l can, in general, be written as

$$M_l = P_l M_l^r P_l^\dagger, \tag{10}$$

where P_l is a unitary diagonal phase matrix, $\text{diag}(1, e^{i\phi_1}, e^{i\phi_2})$, and M_l^r is a real matrix which can be diagonalized by a real orthogonal matrix O_l as

$$M_l^r = O_l M_l^d O_l^T, \tag{11}$$

where the superscript T denotes transposition and $M_l^d = \text{diag}(m_e, m_\mu, m_\tau)$. From Eqs. (10) and (11), the unitary matrix V_l is given by

$$V_l = P_l O_l. \tag{12}$$

Using the invariants $\text{Tr}M_l^r$, $\text{Tr}M_l^{r^2}$, and $\text{Det}M_l^r$ we get the matrix elements f_l, $|e_l|$, and $|b_l|$ as

$$\begin{aligned} f_l &= m_e - m_\mu + m_\tau - 2a_l, \\ |e_l| &= \left(-\frac{(2a_l - m_e + m_\mu)(2a_l - m_e - m_\tau)(2a_l + m_\mu - m_\tau)}{3a_l - m_e + m_\mu - m_\tau}\right)^{1/2}, \\ |b_l| &= \left(\frac{(a_l - m_e)(a_l + m_\mu)(a_l - m_\tau)}{3a_l - m_e + m_\mu - m_\tau}\right)^{1/2}. \end{aligned} \tag{13}$$

Here, a_l has two allowed ranges $(\frac{m_\tau - m_\mu}{2}) < a_l < (\frac{m_\tau + m_e}{2})$ and $(-\frac{m_\mu}{2} < a_l < \frac{m_e}{2})$ for the elements $|e_l|$ and $|b_l|$ to be real. The elements of the diagonalizing matrix O_l can be written in terms of the charged lepton masses m_e, m_μ, m_τ and the charged lepton mass matrix elements a_l, b_l, and e_l. The elements b_l and c_l can be written in terms of a_l, thus leading to a single unknown parameter a_l, and O_l is given by

$$O_l = \begin{pmatrix} \frac{(-e_l^2 - (a_l - m_e)(2a_l + m_\mu - m_\tau))}{A} & \frac{(e_l^2 + (a_l + m_\mu)(2a_l - m_e - m_\tau))}{B} & \frac{(e_l^2 + (2a_l - m_e + m_\mu)(a_l - m_\tau))}{C} \\ \frac{b_l(2a_l + m_\mu - m_\tau)}{A} & \frac{b_l(-2a_l + m_e + m_\tau)}{B} & \frac{b_l(-2a_l + m_e - m_\mu)}{C} \\ \frac{b_l e_l}{A} & -\frac{b_l e_l}{B} & -\frac{b_l e_l}{C} \end{pmatrix}, \tag{14}$$

where A, B, and C are given by

$$\begin{aligned} A = {} & [4a_l^4 + b_l^2(e_l^2 + (m_\mu - m_\tau)^2) - 4a_l^3(2m_e - m_\mu + m_\tau) + (e_l^2 - m_e m_\mu + m_e m_\tau)^2 + a_l^2(4b_l^2 + 4e_l^2 + 4m_e^2 \\ & + (m_\mu - m_\tau)^2 + 8m_e(-m_\mu + m_\tau)) - 2a_l(2b_l^2(-m_\mu + m_\tau) + (2m_e - m_\mu + m_\tau)(e_l^2 + m_e(-m_\mu + m_\tau)))]^{1/2}, \\ B = {} & [4a_l^4 - 4a_l^3(m_e - 2m_\mu + m_\tau) + a_l^2(4b_l^2 + 4e_l^2 - m_e^2 - 8m_e m_\mu + 4m_\mu^2 + 2m_e m_\tau - 8m_\mu m_\tau + m_\tau^2) \\ & + (e_l^2 - m_\mu(m_e + m_\tau))^2 + b_l^2(e_l^2 + (m_e + m_\tau)^2) - 2a_l(2b_l^2(m_e + m_\tau) + (m_e - 2m_\mu + m_\tau)(e_l^2 - m_\mu(m_e + m_\tau))]^{1/2}, \\ C = {} & [4a_l^4 + b_l^2(e_l^2 + (m_e - m_\mu)^2) - 4a_l^3(m_e - m_\mu + 2m_\tau) + (e_l^2 + m_\tau(m_e - m_\tau))^2 + a_l^2(4b_l^2 + 4e_l^2(m_e - m_\mu)^2 \\ & + 8(m_e - m_\mu)m_\tau + 4m_\tau^2) - 2a_l(2b_l^2(m_e - m_\mu) + (m_e - m_\mu + 2m_\tau)(e_l^2 + (m_e - m_\mu)m_\tau))]^{1/2}\}. \end{aligned} \tag{15}$$

If a_l is known, the diagonalizing matrix O_l and the real charged lepton mass matrix M_l^r are fully determined since the charged lepton masses are known. The complex symmetric neutrino mass matrix M_ν is diagonalized by a complex unitary matrix V_ν:

$$M_\nu = V_\nu M_\nu^{\text{diag}} V_\nu^T. \tag{16}$$

The lepton mixing matrix or Pontecorvo-Maki-Nakagawa-Sakata (PMNS) matrix U_{PMNS} [23] is given by

$$U_{\text{PMNS}} = V_l^\dagger V_\nu. \tag{17}$$

The mixing matrix U_{PMNS} consists of three nontrivial CP violating phases: the Dirac phase δ and the two Majorana phases α, β, and the three neutrino mixing angles viz. θ_{12}, θ_{23}, and θ_{13}. The neutrino mixing matrix can be written as the product of two matrices characterizing Dirac-type and Majorana-type CP violation, i.e.,

$$U_{\text{PMNS}} = UP, \tag{18}$$

where U and P [24] are given by

$$U = \begin{pmatrix} c_{12}c_{13} & s_{12}c_{13} & s_{13}e^{-i\delta} \\ -s_{12}c_{23} - c_{12}s_{23}s_{13}e^{i\delta} & c_{12}c_{23} - s_{12}s_{23}s_{13}e^{i\delta} & s_{23}c_{13} \\ s_{12}s_{23} - c_{12}c_{23}s_{13}e^{i\delta} & -c_{12}s_{23} - s_{12}c_{23}s_{13}e^{i\delta} & c_{23}c_{13} \end{pmatrix}, \qquad P = \begin{pmatrix} 1 & 0 & 0 \\ 0 & e^{i\alpha} & 0 \\ 0 & 0 & e^{i(\beta+\delta)} \end{pmatrix}. \tag{19}$$

From Eqs. (16) and (17), the neutrino mass matrix M_ν can be written as

$$M_\nu = P_l O_l U_{\text{PMNS}} M_\nu^{\text{diag}} U_{\text{PMNS}}^T O_l^T P_l^\dagger. \tag{20}$$

A texture zero and an equality in M_ν yield two complex equations

$$m_1 ap + m_2 bqe^{2i\alpha} + m_3 cre^{2i(\beta+\delta)} = 0, \tag{21}$$

$$m_1(a^2 - d^2) + m_2(b^2 - g^2)e^{2i\alpha} + m_3(c^2 - h^2)e^{2i(\beta+\delta)} = 0, \tag{22}$$

where the complex coefficients a, b, c, d, g, h, p, q, and r are given by

$$\begin{aligned}
a &= O_{11}U_{e1} + O_{12}U_{m1} + O_{13}U_{t1},\\
b &= O_{11}U_{e2} + O_{12}U_{m2} + O_{13}U_{t2},\\
c &= O_{11}U_{e3} + O_{12}U_{m3} + O_{13}U_{t3},\\
d &= O_{21}U_{e1} + O_{22}U_{m1} + O_{23}U_{t1},\\
g &= O_{21}U_{e2} + O_{22}U_{m2} + O_{23}U_{t2},\\
h &= O_{21}U_{e3} + O_{22}U_{m3} + O_{23}U_{t3},\\
p &= O_{31}U_{e1} + O_{32}U_{m1} + O_{33}U_{t1},\\
q &= O_{31}U_{e2} + O_{32}U_{m2} + O_{33}U_{t2},\\
r &= O_{31}U_{e3} + O_{32}U_{m3} + O_{33}U_{t3}.
\end{aligned} \tag{23}$$

The two complex Eqs. (21) and (22) can be solved simultaneously to get the following two mass ratios:

$$\begin{aligned}
\frac{m_1}{m_2}e^{-2i\alpha} &= \left(\frac{cr(b^2 - g^2) - bq(c^2 - h^2)}{ap(c^2 - h^2) - cr(a^2 - d^2)}\right),\\
\frac{m_1}{m_3}e^{-2i\beta} &= \left(\frac{bq(c^2 - h^2) - cr(b^2 - g^2)}{ap(b^2 - g^2) - bq(a^2 - d^2)}\right)e^{2i\delta}.
\end{aligned} \tag{24}$$

It is useful to enumerate the number of parameters in Eq. (24). The nine parameters including the three neutrino mixing angles ($\theta_{12}, \theta_{23}, \theta_{13}$), three neutrino mass eigenvalues (m_1, m_2, m_3), two Majorana phases (α, β), and one Dirac-type CP violating phase (δ) come from the neutrino sector and the four parameters including the three charged lepton masses (m_e, m_μ, m_τ) and a_l come from the charged lepton sector, thus totalling 13 parameters. The three charged lepton masses are known [25]

$$\begin{aligned}
m_e &= 0.510\,998\,910 \text{ MeV},\\
m_\mu &= 105.658\,367 \text{ MeV},\\
m_\tau &= 1776.84 \text{ MeV}.
\end{aligned} \tag{25}$$

The masses m_2 and m_3 can be calculated from the mass-squared differences Δm_{12}^2 and Δm_{23}^2 using the relations

$$m_2 = \sqrt{m_1^2 + \Delta m_{12}^2} \tag{26}$$

and

$$m_3 = \sqrt{m_2^2 + \Delta m_{23}^2}. \tag{27}$$

Using the known values of the two mass-squared differences and the two mixing angles, we can constrain the other parameters. The parameters δ and a_l are varied uniformly within their full possible ranges while θ_{13} is varied uniformly up to its upper bound given by CHOOZ [20]. Thus, we are left with three unknown parameters viz. m_1, α, β. The magnitudes of the two mass ratios are given by

$$\sigma = \left|\frac{m_1}{m_2}e^{-2i\alpha}\right|, \tag{28}$$

and

$$\rho = \left|\frac{m_1}{m_3}e^{-2i\beta}\right|, \tag{29}$$

while the CP violating Majorana phases are given by

$$\alpha = -\frac{1}{2}\arg\left(\frac{cr(b^2 - g^2) - bq(c^2 - h^2)}{ap(c^2 - h^2) - cr(a^2 - d^2)}\right), \tag{30}$$

$$\beta = -\frac{1}{2}\arg\left(\frac{bq(c^2 - h^2) - cr(b^2 - g^2)}{ap(b^2 - g^2) - bq(a^2 - d^2)}\right)e^{2i\delta}. \tag{31}$$

Since, Δm_{12}^2 and Δm_{23}^2 are known experimentally, the values of mass ratios (ρ, σ) from Eqs. (28) and (29) can be used to calculate m_1. This can be achieved by inverting Eqs. (26) and (27) to obtain the two values of m_1 viz.

$$m_1 = \sigma\sqrt{\frac{\Delta m_{12}^2}{1 - \sigma^2}}, \tag{32}$$

and

$$m_1 = \rho\sqrt{\frac{\Delta m_{12}^2 + \Delta m_{23}^2}{1 - \rho^2}}. \tag{33}$$

We vary the oscillation parameters within their known experimental ranges. The two values of m_1 obtained from the mass ratios ρ and σ, respectively, must be equal to within the errors of the oscillation parameters for this hybrid texture to be phenomenologically viable.

This class of hybrid texture has both normal and inverted hierarchical mass spectrum. We get some interesting predictions for other parameters for each hierarchy which are to be probed in the forthcoming neutrino oscillation experiments. For inverted hierarchy, a small range of the two Majorana-type CP violating phases α and β is allowed at 3σ. It can be seen from Fig. 1(a) that α can take the values 0° or 180° while β is constrained to the range (-25°)–(25°). There exists a clear bound on the reactor neutrino mixing angle ($\theta_{13} > 1^\circ$) while the Dirac-type CP violating phase δ is disallowed between 30°–130° [Fig. 1(b)]. There exists an upper bound of 0.2 eV on the

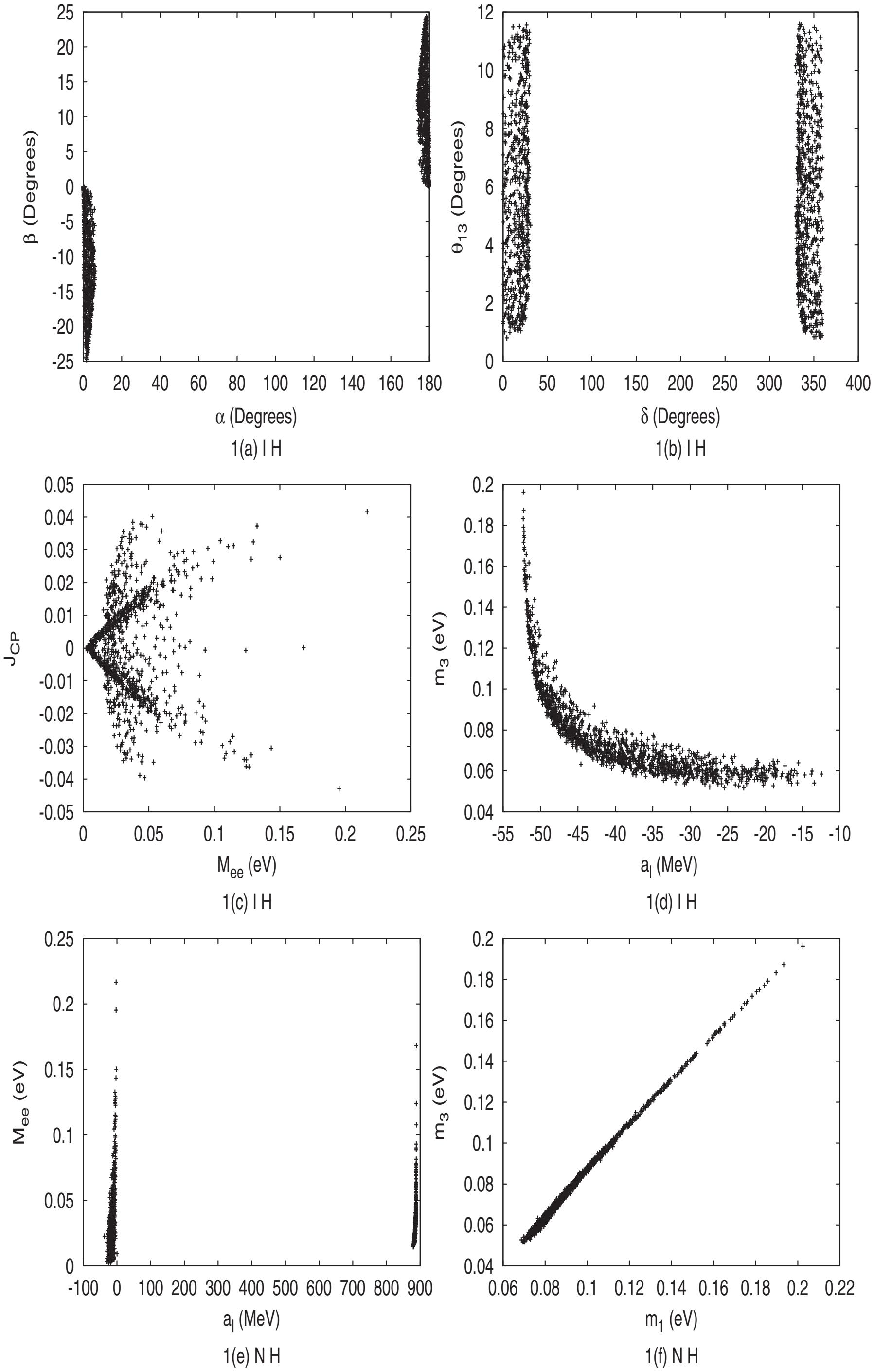

FIG. 1. Correlation plots for class I.

effective Majorana mass M_{ee} and the allowed range of Jarlskog rephasing invariant J_{CP} is (-0.04)–(0.04) [Fig. 1(c)]. The range of the unknown parameter a_l allowed by the current neutrino oscillation data is $[(-53) \leq a_l \leq (-10)]$ MeV as depicted in Fig. 1(d). For normal hierarchy an upper bound of 0.25 eV is obtained for the effective Majorana mass M_{ee}. Two highly constrained regions of parameter space are obtained for the free parameter a_l as depicted in Fig. 1(e). All the other hybrid texture structures in this class have the same physical implications.

B. Class II

Here, we study the phenomenological implications of the parallel hybrid texture structure for the charged lepton mass matrix and the neutrino mass matrix with equality between (2, 2) and (3, 3) elements and a texture zero at the (1, 1) position (case IIA):

$$M_l = \begin{pmatrix} 0 & b_l & c_l \\ b_l^* & d_l & e_l \\ c_l^* & e_l^* & d_l \end{pmatrix}, \qquad M_\nu = \begin{pmatrix} 0 & b_\nu & c_\nu \\ b_\nu & d_\nu & e_\nu \\ c_\nu & e_\nu & d_\nu \end{pmatrix}. \tag{34}$$

We consider the phases appearing in the charged lepton mass matrix to be factorizable since it is not possible to completely remove all the phases from this type of charged lepton mass matrix where both equality and zero appear along the diagonal entries. We perform analysis similar to class I for this hybrid texture. Using the conditions from three invariants, we get the matrix elements d_l, $|b_l|$, and $|c_l|$ to be

$$\begin{aligned} d_l &= \frac{m_e - m_\mu + m_\tau}{2}, \\ |b_l| &= \frac{(-4e_l^2(m_e - m_\mu + m_\tau) + (m_e - m_\mu - m_\tau)(m_e + m_\mu - m_\tau)(m_e + m_\mu + m_\tau))}{e_l X}, \\ |c_l| &= \frac{1}{X}, \end{aligned} \tag{35}$$

where

$$X = 4\left[\left(-8e_l^2 + \frac{1}{e_l}((2e_l - m_e - m_\mu - m_\tau)(2e_l + m_e - m_\mu - m_\tau)(2e_l + m_e + m_\mu - m_\tau)(2e_l - m_e - m_\mu + m_\tau) \times (2e_l - m_e + m_\mu + m_\tau)(2e_l + m_e + m_\mu + m_\tau))^{1/2}\right) + 2(m_e^2 + 2m_e(m_\mu - m_\tau) + (m_\mu + m_\tau)^2)\right]^{1/2}. \tag{36}$$

Here, e_l should be in the range $\frac{(m_\tau - m_\mu - m_e)}{2} < e_l < \frac{(m_\tau + m_\mu - m_e)}{2}$ for the elements b_l and c_l to be real. The elements of the diagonalizing matrix O_l can be written in terms of the charged lepton masses and the parameters e_l, b_l, and c_l. The parameters b_l and c_l are the functions of e_l [Eq. (35)], thus leading to a single unknown parameter e_l, and O_l is given by

$$O_l = \begin{pmatrix} -\frac{(2b_l e_l + c_l(m_e + m_\mu - m_\tau))}{A} & \frac{(2b_l e_l - c_l(m_e + m_\mu + m_\tau))}{B} & \frac{(2b_l e_l + c_l(-m_e + m_\mu + m_\tau))}{D} \\ -\frac{2(b_l c_l + e_l m_e)}{A} & \frac{2(b_l c_l - e_l m_\mu)}{B} & \frac{2(b_l c_l + e_l m_\tau)}{D} \\ \frac{(2b_l^2 - m_e(m_e + m_\mu - m_\tau))}{A} & \frac{(-2b_l^2 + m_\mu(m_e + m_\mu + m_\tau))}{B} & \frac{(-2b_l^2 + m_\tau(-m_e + m_\mu + m_\tau))}{D} \end{pmatrix}, \tag{37}$$

where A, B, D are given by

$$\begin{aligned} A &= [4b_l^4 + 4b_l^2(c_l^2 + e_l^2 - m_e(m_e + m_\mu - m_\tau)) + m_e^2(4e_l^2 + (m_e + m_\mu - m_\tau)^2) + c_l^2(m_e + m_\mu - m_\tau)^2 \\ &\quad + 4b_l c_l e_l(3m_e + m_\mu - m_\tau)]^{1/2}, \\ B &= [4b_l^4 + c_l^2(m_e + m_\mu + m_\tau)^2 - 4b_l c_l e_l(m_e + 3m_\mu + m_\tau) + 4b_l^2(c_l^2 + e_l^2 - m_\mu)(m_e + m_\mu + m_\tau) \\ &\quad + m_\mu^2(4e_l^2 + (m_e + m_\mu + m_\tau))^2]^{1/2}, \\ D &= [4b_l^4 + c_l^2(-m_e + m_\mu + m_\tau)^2 + 4b_l c_l e_l(-m_e + m_\mu + 3m_\tau) + 4b_l^2(c_l^2 + e_l^2 + m_\tau(m_e - m_\mu - m_\tau) \\ &\quad + m_\tau^2(4e_l^2 + (-m_e + m_\mu + m_\tau))^2]^{1/2}. \end{aligned} \tag{38}$$

This structure of hybrid texture of M_ν results in two complex equations,

$$m_1 a^2 + m_2 b^2 e^{2i\alpha} + m_3 c^2 e^{2i(\beta+\delta)} = 0, \tag{39}$$

$$m_1(d^2 - p^2) + m_2(g^2 - q^2)e^{2i\alpha} + m_3(h^2 - r^2)e^{2i(\beta+\delta)} = 0, \tag{40}$$

where the complex coefficients a, b, c, d, g, h, p, q, and r have the same form as given in Eq. (23). The mass ratios can be found from the two complex Eqs. (39) and (40) and are given by

$$\begin{aligned} \frac{m_1}{m_2} e^{-2i\alpha} &= \left(\frac{c^2(g^2 - q^2) - b^2(h^2 - r^2)}{a^2(h^2 - r^2) - c^2(d^2 - p^2)}\right), \\ \frac{m_1}{m_3} e^{-2i\beta} &= \left(\frac{b^2(h^2 - r^2) - c^2(g^2 - q^2)}{a^2(g^2 - q^2) - b^2(d^2 - p^2)}\right) e^{2i\delta}. \end{aligned} \tag{41}$$

The absolute values of Eq. (41) yield the two mass ratios $(\frac{m_1}{m_2})$ and $(\frac{m_1}{m_3})$ while the arguments of these equations give us information about the two Majorana-type CP violating phases α and β as shown in detail earlier. By equating the two values of m_1 to within the errors of the oscillation parameters we obtain interesting implications for this hybrid texture.

Specifically, both normal and inverted hierarchies are allowed for this class. For inverted hierarchy, the Majorana-type CP violating phase α is constrained to the range 75°–105° [Fig. 2(a)]. In this case, an upper as well as a lower bound is obtained for effective Majorana mass, $(0.01 < M_{ee} < 0.08)$ eV and a highly constrained range (880–940) MeV for the free parameter e_l is allowed as can be seen from Fig. 2(b). For normal hierarchy M_{ee} is constrained to be less than 0.1 eV [Fig. 2(c)].

C. Class III

Another class of hybrid textures which leads to interesting implications is when the texture zero is at the (1, 1) position while (1, 2) and (1, 3) elements are equal (case IIIA). Here,

$$M_l = \begin{pmatrix} 0 & b_l & b_l \\ b_l^* & d_l & e_l \\ b_l^* & e_l^* & f_l \end{pmatrix}, \qquad M_\nu = \begin{pmatrix} 0 & b_\nu & b_\nu \\ b_\nu & d_\nu & e_\nu \\ b_\nu & e_\nu & f_\nu \end{pmatrix}. \tag{42}$$

Using the invariants, we get the matrix elements $|b_l|$, d_l and f_l as

$$\begin{aligned} |b_l| &= \sqrt{\frac{m_e m_\mu m_\tau}{(-2e_l + m_e - m_\mu + m_\tau)}}, \\ d_l &= \frac{1}{2}\left[\frac{(2e_l - m_e - m_\mu - m_\tau)(2e_l + m_e + m_\mu - m_\tau)(2e_l - m_e + m_\mu + m_\tau)}{(-2e_l + m_e - m_\mu + m_\tau)}\right]^{1/2} + \frac{1}{2}(m_e - m_\mu + m_\tau), \\ f_l &= m_e - m_\mu + m_\tau - d_l. \end{aligned} \tag{43}$$

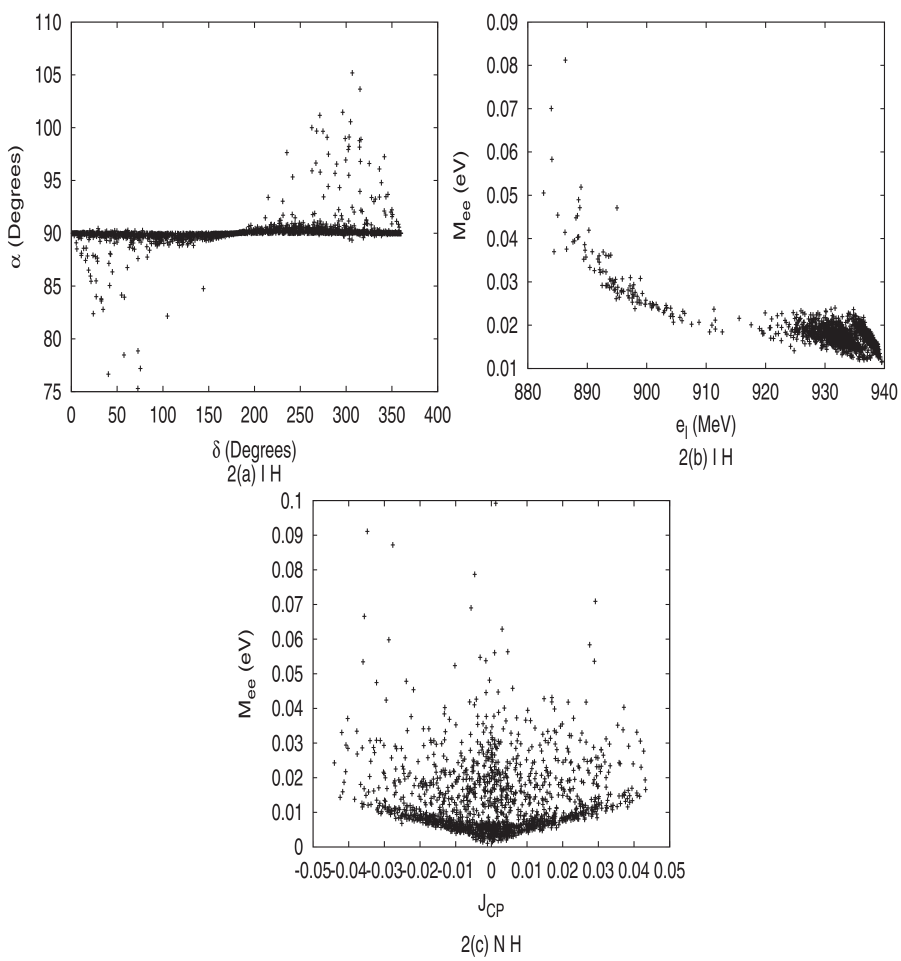

FIG. 2. Correlation plots for class II.

The free parameter e_l is constrained to the range $(\frac{(m_e-m_\mu-m_\tau)}{2}) < e_l < (\frac{(m_\tau-m_\mu-m_e)}{2})$ for the element b_l to be real. The orthogonal diagonalizing matrix O_l can be written in terms of the charged lepton masses and charged lepton mass matrix elements:

$$O_l = \begin{pmatrix} -\frac{(e_l^2+(d_l-m_e)(d_l+m_\mu-m_\tau))}{A} & \frac{e_l^2+(d_l+m_\mu)(d_l-m_e+m_\tau)}{B} & \frac{-(e_l^2+(d_l-m_e+m_\mu)(d_l-m_\tau))}{D} \\ \frac{b_l(d_l+e_l+m_\mu-m_\tau)}{A} & \frac{b_l(-d_l-e_l+m_e+m_\tau)}{B} & \frac{b_l(d_l+e_l-m_e+m_\mu)}{D} \\ \frac{b_l(-d_l+e_l+m_e)}{A} & \frac{b_l(d_l-m_e+m_\mu)}{B} & \frac{b_l(-d_l+e_l+m_\tau)}{D} \end{pmatrix}, \tag{44}$$

where A, B, and D are given by

$$\begin{aligned} A &= [(e_l^2 + (d_l - m_e)(d_l + m_\mu - m_\tau))^2 + b_l^2(2d_l^2 + 2e_l^2 + m_e^2 + (m_\mu - m_\tau)^2 + 2e_l(m_e + m_\mu - m_\tau) \\ &\quad - 2d_l(m_e - m_\mu + m_\tau))], \\ B &= [(e_l^2 + (d_l + m_\mu)(d_l - m_e - m_\tau))^2 + b_l^2(2d_l^2 + 2e_l^2 + m_\mu^2 + (m_e + m_\tau)^2 - 2d_l(m_e - m_\mu + m_\tau) \\ &\quad - 2e_l(m_e + m_\mu - m_\tau))]^{1/2}, \\ D &= [(e_l^2 + (d_l - m_e + m_\mu)(d_l - m_\tau))^2 + b_l^2(2d_l^2 + 2e_l^2 + m_\tau^2 + (m_e - m_\mu)^2 - 2d_l(m_e - m_\mu + m_\tau) \\ &\quad + 2e_l(-m_e + m_\mu + m_\tau))]^{1/2}. \end{aligned} \tag{45}$$

The simultaneous existence of a texture zero and an equality in M_ν leads to the following complex equations:

$$m_1a^2 + m_2b^2e^{2i\alpha} + m_3c^2e^{2i(\beta+\delta)} = 0, \tag{46}$$

$$m_1(ad - ap) + m_2(bg - bq)e^{2i\alpha} + m_3(ch - cr)e^{2i(\beta+\delta)} = 0. \tag{47}$$

The complex coefficients are given in Eq. (23). Using these two complex equations we find the two mass ratios to be

$$\begin{aligned} \frac{m_1}{m_2}e^{-2i\alpha} &= \left(\frac{c^2(bg - bq) - b^2(ch - cr)}{a^2(ch - cr) - c^2(ad - ap)}\right), \\ \frac{m_1}{m_3}e^{-2i\beta} &= \left(\frac{b^2(ch - cr) - c^2(bg - bq)}{a^2(bg - bq) - b^2(ad - ap)}\right)e^{2i\delta}. \end{aligned} \tag{48}$$

We perform a similar numerical analysis for this class and find that it is consistent with normal hierarchy only. A stringent bound on θ_{13} is obtained. There exists a lower bound of 4° on the 1–3 mixing angle [Fig. 3(a)]. The unknown parameter e_l has two allowed regions viz. [(−960) − (−680)] MeV and (430–830) MeV. The effective Majorana mass is constrained to be less than 0.0045 eV for both regions of e_l [Fig. 3(b)].

IV. REMAINING VIABLE CLASSES OF HYBRID TEXTURES

The remaining phenomenologically viable classes are IV, V, VI, and VII. As for the classes discussed so far, the condition of a texture zero and an equality in M_ν results in two complex equations given in Table II. The two mass ratios obtained for these hybrid textures are given in Table III. When we apply our numerical analysis on all these classes we find that they have normal hierarchical mass spectra.

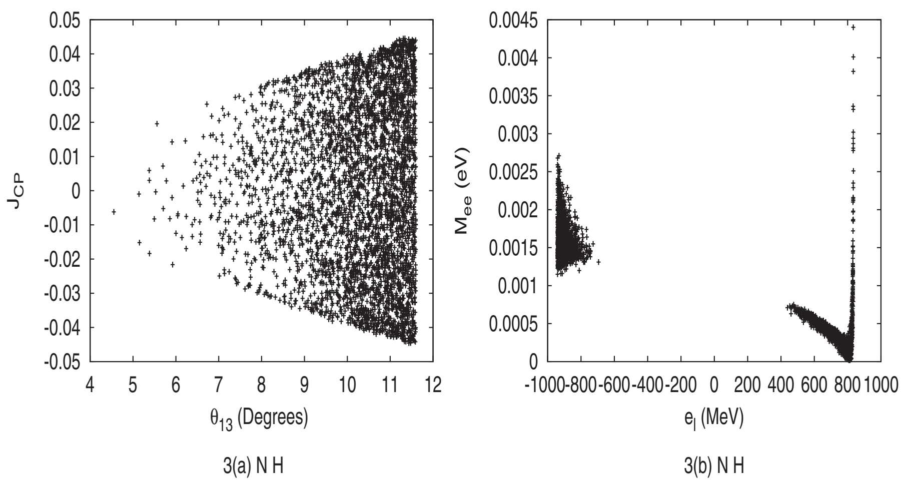

FIG. 3. Correlation plots for class III.

TABLE II. Complex equations for remaining viable cases.

Case	Complex equations
IVA	$m_1 d^2 + m_2 g^2 e^{2i\alpha} + m_3 h^2 e^{2i(\beta+\delta)} = 0$
	$m_1(a^2 - ad) + m_2(b^2 - bg)e^{2i\alpha} + m_3(c^2 - ch)e^{2i(\beta+\delta)} = 0$
VA	$m_1 p^2 + m_2 q^2 e^{2i\alpha} + m_3 r^2 e^{2i(\beta+\delta)} = 0$
	$m_1(a^2 - ad) + m_2(b^2 - bg)e^{2i\alpha} + m_3(c^2 - ch)e^{2i(\beta+\delta)} = 0$
VIA	$m_1 d^2 + m_2 g^2 e^{2i\alpha} + m_3 h^2 e^{2i(\beta+\delta)} = 0$
	$m_1(a^2 - dp) + m_2(b^2 - gq)e^{2i\alpha} + m_3(c^2 - hr)e^{2i(\beta+\delta)} = 0$
VIIA	$m_1 ap + m_2 bqe^{2i\alpha} + m_3 cre^{2i(\beta+\delta)} = 0$
	$m_1(a^2 - ad) + m_2(p^2 - pg)e^{2i\alpha} + m_3(b^2 - bh)e^{2i(\beta+\delta)} = 0$

TABLE III. Mass ratios for remaining viable cases.

Case	$\frac{m_1}{m_3} e^{-2i\beta}$	$\frac{m_1}{m_2} e^{-2i\alpha}$
IVA	$\left(\frac{g^2(c^2-ch)-h^2(b^2-bg)}{d^2(b^2-bg)-g^2(a^2-ad)}\right)$	$\left(\frac{h^2(b^2-bg)-g^2(a^2-ad)}{d^2(c^2-ch)-h^2(a^2-ad)}\right)e^{2i\delta}$
VA	$\left(\frac{q^2(c^2-ch)-r^2(b^2-bg)}{p^2(b^2-bg)-q^2(a^2-ad)}\right)$	$\left(\frac{r^2(b^2-bg)-q^2(c^2-ch)}{p^2(c^2-ch)-r^2(a^2-ad)}\right)e^{2i\delta}$
VIA	$\left(\frac{g^2(c^2-hr)-h^2(b^2-gq)}{d^2(b^2-gq)-g^2(a^2-dp)}\right)$	$\left(\frac{h^2(b^2-gq)-g^2(c^2-hr)}{d^2(c^2-hr)-h^2(a^2-dp)}\right)e^{2i\delta}$
VIIA	$\left(\frac{bq(hb-b^2)-cr(gp-p^2)}{ap(gp-p^2)-bq(da-a^2)}\right)$	$\left(\frac{cr(gp-p^2)-bq(hb-b^2)}{ap(hb-b^2)-cr(da-a^2)}\right)e^{2i\delta}$

For class IV a constrained region [(−55)–(165)] MeV for the free parameter e_l along with an upper bound of 0.035 eV on effective Majorana mass M_{ee} is obtained which can be seen from Fig. 4(a). For class V, two regions of solutions (−100–0) MeV and (833–930) MeV are obtained for the free parameter a_l. There exists an upper bound of 0.012 eV on the effective Majorana mass (M_{ee} [Fig. 4(b)]). There is a strong correlation between the two phases β and δ as can be seen from Fig. 4(c). For class VI a stringent bound on effective Majorana mass is obtained: ($0.008 < M_{ee} < 0.04$) eV [Fig. 4(d)]. Class VII is only marginally allowed since only 10–15 points are allowed whereas the total number of points generated in our numerical analysis is 10^7.

V. CONCLUSIONS

We presented a comprehensive phenomenological analysis for the parallel hybrid texture structures of the charged lepton and the neutrino mass matrices. These parallel hybrid texture structures cannot be obtained from arbitrary Hermitian charged lepton and complex symmetric neutrino mass matrices through weak basis transformations and thus have physical implications. All the possible 60 hybrid texture structures are grouped into 12 classes

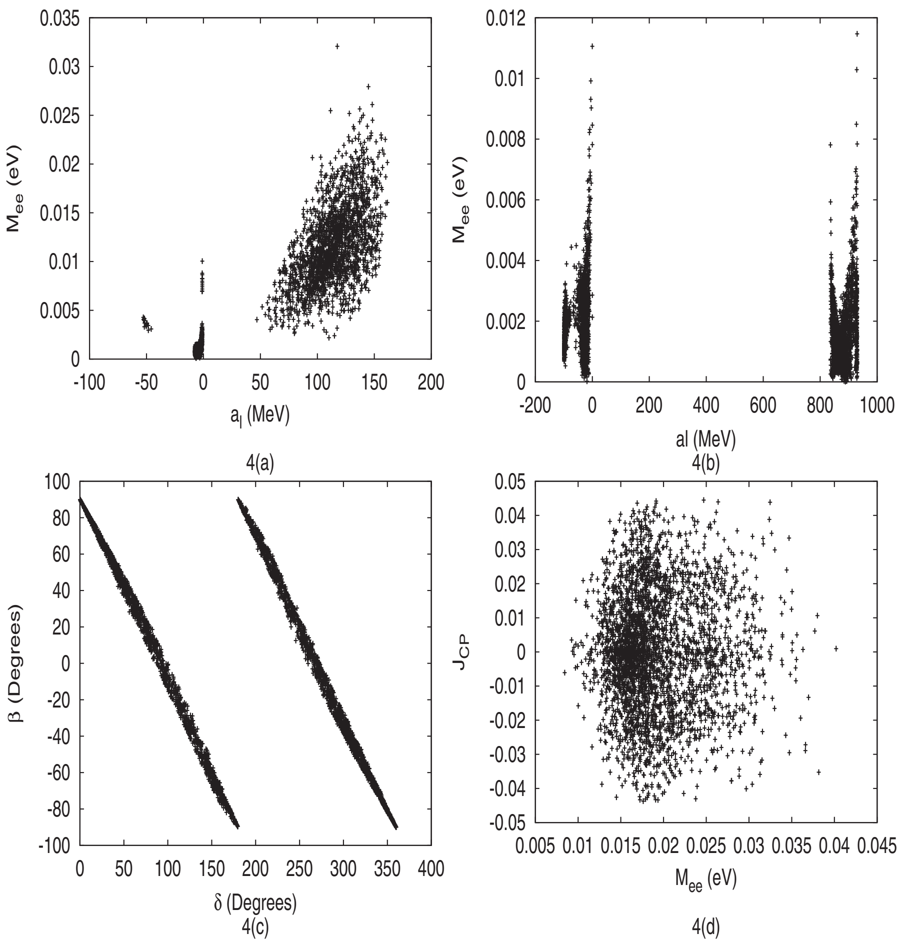

FIG. 4. Correlation plots for classes IV, V, and VI.

using the permutation matrices. All textures in a class have the same physical implications. Six out of total 12 classes are found to be phenomenologically viable and have interesting implications while class VII is only marginally allowed. The remaining five classes of hybrid textures are phenomenologically disallowed. For each class, we obtained the allowed range for the only free parameter from the charged lepton sector. Predictions for the 1–3 mixing angle, the Dirac-type and Majorana-type *CP* violating phases are obtained for some of the allowed hybrid texture structures. We also obtained bounds on the effective Majorana mass for all the allowed hybrid texture structures. The study of these parameters is significant as they are expected to be probed in the forthcoming experiments.

ACKNOWLEDGMENTS

The research work of S. D. is supported by the University Grants Commission, Government of India, Grant No. 34-32/2008 (SR). S. G. and R. R. G. acknowledge the financial support provided by the Council for Scientific and Industrial Research (CSIR), Government of India.

[1] Paul H. Frampton, Sheldon L. Glashow, and Danny Marfatia, Phys. Lett. B **536**, 79 (2002); Bipin R. Desai, D. P. Roy, and Alexander R. Vaucher, Mod. Phys. Lett. A **18**, 1355 (2003).
[2] Zhi-zhong Xing, Phys. Lett. B **530**, 159 (2002).
[3] Wanlei Guo and Zhi-zhong Xing, Phys. Rev. D **67**, 053002 (2003).
[4] Alexander Merle and Werner Rodejohann, Phys. Rev. D **73**, 073012 (2006); S. Dev and Sanjeev Kumar, Mod. Phys. Lett. A **22**, 1401 (2007).
[5] S. Dev, Sanjeev Kumar, Surender Verma, and Shivani Gupta, Nucl. Phys. **B784**, 103 (2007).
[6] S. Dev, Sanjeev Kumar, Surender Verma, and Shivani Gupta, Phys. Rev. D **76**, 013002 (2007).
[7] G. C. Branco, R. Gonzalez Felipe, F. R. Joaquim, and T. Yanagida, Phys. Lett. B **562**, 265 (2003); Bhag C. Chauhan, Joao Pulido, and Marco Picariello, Phys. Rev. D **73**, 053003 (2006).
[8] Xiao-Gang He and A. Zee, Phys. Rev. D **68**, 037302 (2003).
[9] E. I. Lashin and N. Chamoun, Phys. Rev. D **78**, 073002 (2008); **80**, 093004 (2009).
[10] S. Dev, Surender Verma, Shivani Gupta, and R. R. Gautam, Phys. Rev. D **81**, 053010 (2010).
[11] H. C. Goh, R. N. Mohapatra, and Siew-Phang Ng, Phys. Rev. D **68**, 115008 (2003).
[12] M. Frigerio, S. Kaneko, E. Ma, and M. Tanimoto, Phys. Rev. D **71**, 011901 (2005).
[13] S. Kaneko, H. Sawanaka, and M. Tanimoto, J. High Energy Phys. 08 (2005) 073; S. Dev, Surender Verma, and Shivani Gupta, Phys. Lett. B **687**, 53 (2010).
[14] C. Jarlskog, Phys. Rev. Lett. **55**, 1039 (1985).
[15] H. V. Klapdor-Kleingrothaus, Nucl. Phys. B, Proc. Suppl. **145**, 219 (2005).
[16] C. Arnaboldi *et al.*, Nucl. Instrum. Methods Phys. Res., Sect. A **518**, 775 (2004).
[17] C. Arnaboldi *et al.* (CUORICINO Collaboration), Phys. Lett. B **584**, 260 (2004).
[18] I. Abt *et al.* (GERDA Collaboration), arXiv:hep-ex/0404039.
[19] X. Sarazin *et al.*, arXiv:hep-ex/0006031.
[20] G. L. Fogli *et al.*, Phys. Rev. D **78**, 033010 (2008).
[21] G. C. Branco, D. Emmanuel-Costa, R. González Felipe, and H. Serôdio, Phys. Lett. B **670**, 340 (2009).
[22] G. Ahuja, S. Kumar, M. Randhawa, M. Gupta, and S. Dev, Phys. Rev. D **76**, 013006 (2007); S. Dev, Sanjeev Kumar, Surender Verma, and Shivani Gupta, Mod. Phys. Lett. A **24**, 2251 (2009).
[23] B. Pontecorvo Zh. Eksp. Teor. Fiz. **33**, 549 (1957) [Sov. Phys. JETP **33**, 429 (1957)]; Zh. Eksp. Teor. Fiz. **34**, 247 (1958) [Sov. Phys. JETP **7**, 172 (1958)]; Zh. Eksp. Teor. Fiz. **53**, 1717 (1967) [Sov. Phys. JETP **26**, 984 (1968)]; Z. Maki, M. Nakagawa, and S. Sakata, Prog. Theor. Phys. **28**, 870 (1962).
[24] G. L. Fogli *et al.*, Prog. Part. Nucl. Phys. **57**, 742 (2006).
[25] C. Amsler *et al.*, Phys. Lett. B **667**, 1 (2008).